Annual Variation of Temperature Field and Heat Transfer under Heated Ground Surfaces: Slab-on-Grade Floor Heat Loss Calculations

T. Kusuda **O. Piet** **J.W. Bean**
ASHRAE Fellow

ABSTRACT

Seasonal subsurface ground temperature profile and surface heat-transfer were determined for the condition when one and more than one region of the earth's surface temperature was disturbed. The analysis was conducted by numerical integration using a closed form solution based on the Green's function. Monthly profiles of earth temperature isotherms under a house of 20 ft by 20 ft (6.1 m by 6.1 m) floor area and under a group of six houses near a wooded area are presented. The heat losses calculated from this approach for square slabs of various sizes were compared with those derived from the recent analytical solution of Delsante et al.

One of the most critical factors for the heat-transfer calculation is the temperature transition across the perimeter zone of the slab. The Delsante solution and the numerical calculation showed good agreement when the numerical calculation was made for a 6 in. linear temperature transition zone. Also included is a simplified slab-on-grade heat-transfer calculation procedure suitable for the microcomputer. This procedure was based on the Delsante's Fourier Transform Integral extending over the perimeter zone where the temperature transition takes place.

INTRODUCTION

The subsurface temperature of the earth undergoing a seasonal cycle depends upon the surface temperature, the thermal diffusivity, and the distance from the surface. A well-known equation for the natural earth temperature is:[1]

$$T_\infty = T_g + \sum_{i=1}^{N} A_i e^{-z\sqrt{\frac{\omega_i}{2\alpha}}} \sin\left(\omega_i t + z\sqrt{\frac{\omega_i}{2\alpha}} + \xi_i\right) \qquad (1)$$

where

T_∞ : undisturbed earth temperature

T_g : annual average surface temperature

A_i : amplitude of the surface temperature, surface temperature variation

z : depth from the surface

Tamami Kusuda, Group Leader, the National Bureau of Standards, Gaithersburg, Maryland.

O. Piet, Guest Worker from École Nationale des Ponts et Chaussées, France.

J. W. Bean, Mathematician, the National Bureau of Standards, Gaithersburg, Maryland.

The Lachenbruch solution for this boundary condition can be expressed as

$$T(x,y,z,t) = \frac{1}{2\pi} \iint_{\Omega} [T_B + (T_C - T_A)L]\, d\Omega \tag{5}$$

where

Ω is the solid angle subtended by the surface segment S above the subsurface point at x, y, z, for which the temperature is calculated, and where

$$d\Omega = \frac{z\,dx'dy'}{r^3} \tag{6}$$

$$L = e^{-\lambda} \quad \sin(wt-\lambda) + \lambda[\cos(wt-\lambda) + \sin(wt-\lambda)] \tag{7}$$

and

$$\lambda = r\sqrt{\frac{\omega}{2\alpha}} \tag{8}$$

Numerical Calculation Procedure

A computer program was developed to determine the soil temperature profile under the ground surface, using the Lachenbruch integral over an elementary rectangular surface segment. The program is called HEATPATCH and can simulate the condition whereby more than one region is disturbed at the ground surface, each disturbance having seasonal cycles different from the naturally exposed outdoor surface.

In this computer program, the ground surface is broken into a rectangular grid, and each of the disturbed areas is prescribed by the respective x and y coordinates of its boundary. Within a given boundary, surface temperature may vary as a spatial function. Fig. 1 illustrates typical surface grid design, where six of the heated patches of 20 ft by 20 ft square represent slab floors of houses located next to a large patch that represents forest. The subsurface soil temperature can then be computed by superposing temperature solutions due to each of the seven in the surface. Assuming that $T_B(x,y)$ and $T_C(x,y)$ are constant over a finite rectangular segment, $\Delta x\, \Delta y$, and performing the integration over the segment designated by (i,j), Eq 5 may be approximated by

$$T(x,y,z,t) = \frac{1}{2\pi} \sum_{i}^{M} \sum_{j}^{N} T_{Bij} + (T_{Cij} - T_A)L_{ij}\ \Delta\Omega_{ij} \tag{9}$$

where

Each of the variables with subscripts i and j is evaluated at a finite difference grid x_i and y_j. The $\Delta\Omega$ may be determined by integration of Eq 6 over a rectangular element of point, sides Δx and Δy, resulting in

$$\begin{aligned} \Delta\Omega = {} & G\left(x-x',\ y-y',\ \frac{\Delta x}{2},\ \frac{\Delta y}{2}\right) \\ & - G\left(x-x',\ y-y',\ \frac{-\Delta x}{2},\ \frac{\Delta y}{2}\right) \\ & - G\left(x-x',\ y-y',\ \frac{\Delta x}{2},\ \frac{-\Delta y}{2}\right) \\ & - G\left(x-x',\ y-y',\ \frac{-\Delta x}{2},\ \frac{-\Delta y}{2}\right) \end{aligned} \tag{10}$$

where

$$G(x,y,a,b) = \tan^{-1}\left[\frac{(x+a)(y+b)}{z\sqrt{z^2 + (x+a)^2 + (y+b)^2}}\right] \tag{11}$$

In order to study the subsurface temperature distribution in the form of isotherms, the earth temperature is calculated for any set of specified points below the earth surface, such as a cross section along the centerline of the slab, along a slab edge, or along a diagonal.

α : thermal diffusivity of the earth

ξ_1 : phase angle or time decay

ω_1 : angular frequency of the 1th harmonics of the surface temperature variation

N : total number of harmonics, usually N=1 for annual cycle

The equation shows that surface temperature fluctuation will quickly diminish at a distance greater than 2 ft (z = 2 ft or 0.61 m) unless the periods of harmonics are extremely large (more than 24 hours). When the segment of the earth's surface is covered by forest, building, or pavement, the surface temperature of that segment experiences a different annual temperature cycle than the natural or uncovered region, or the surface temperature is disturbed. This surface temperature disturbance would influence the subsurface temperature profile, the extent of which depends upon the area of the disturbance, the temperature of the disturbance, and soil thermal diffusivity. For a long-term disturbance, such as that due to the erection of a building, paving, or vegetation, earth temperature calculation for the annual cycle is of the most interest. From the ecological point of view, it is important to know the influence of the disturbance, which will be felt far outside of the disturbed area. In the study of the heating of buildings, it is also important to know the magnitude of the floor heat loss to the ground as a function of the season. In spite of the noteworthy work of numerous researchers, comprehensive analysis of seasonal fluctuation of earth temperature for the heated ground surface has not been available.[1-9] This is because of the complexity of the three-dimensional and transient heat conduction problem that characterizes the ground heat-transfer analysis.

The purpose of this paper is to describe subsurface temperature variation under disturbed ground surface(s) obtained by the Green's function technique, which was introduced by Lachenbruch.[3] Heat loss from the slab-on-grade floor was determined and compared against the results obtained by analytical solutions of Delsante et al.[9] Also presented in this paper is a simplified slab-on-grade heat-loss calculation procedure based upon the comparative study between the solution developed herein and the Delsante solution.

Lachenbruch Solution

According to Carslaw and Jaegger,[10] the basic equation that described the underground temperature affected by the surface temperature disturbance is

$$T(x,y,z,t) = \frac{z}{(\sqrt{4\pi\alpha})^3} \int_0^t \left[\iint_S \frac{T(x',y',t')}{(\sqrt{t-t'})^5} e^{\frac{-r^2}{4\alpha t(-t')}} dx'dy' \right] dt' \qquad (2)$$

where

α = thermal diffusivity of earth

$T(x',y',t')$ = ground surface temperature at z = 0

x',y',t' = arbitrary space and time coordinates for the surface region S

$r^2 = (x-x')^2 + (y-y')^2 + z^2$

Lachenbruch[3] applied this formula for the heated slab with a surface temperature cycle having an angular frequency of ω such that

$$T(x',y',t') = T_B(x',y') + T_C(x',y') \sin \omega t' \qquad (3)$$

over a segment S and

$$T(x',y',t) = T_A \sin \omega t' \qquad (4)$$

outside the area S.

After the subsurface temperature at a depth, ℓ, and position x, y is determined, the surface heat flow can be approximated by

$$q = k[T(x,y,o,t) - T(x,y,\ell,t)]/\ell \qquad (12)$$

where

k = thermal conductivity of soil

The choice of the best depth parameter, ℓ, in the calculation of surface heat-transfer by Eq 12 depends upon the type of temperature distribution over the disturbed region. If there is a very abrupt temperature transition, as in the case of a heated slab floor during the winter, the temperature profiles near the perimeter of the slab have steep gradients in directions normal to the depth. In this case, ℓ must be chosen small enough to account for this edge effect. In the extreme case, if the surface temperature transition from the slab to the exposed outdoor surface is a step function, this results in an infinitely large heat loss at the edge. In actual situations, however, slab surface temperature would be expected to change rather gradually from the indoor condition to the outdoor condition, as is shown in Fig. 2 over a designated perimeter.

The two different types of transition temperature profiles shown in Fig. 2 were studied: the first is a linear change, while the second is a smooth transition representing continuous derivatives. It was found that these two different transitional temperature profiles yield virtually identical results. Only the linear transition is therefore considered in the subsequent analyses.

The HEATPATCH program may also be used to examine various surface and temperature configurations. A number of variations are possible:

1. The size and shape of the disturbed surface segments (or heated patches) can be varied.

2. The number of the heated patches can be varied.

3. Each of the patches can assume an independent mean temperature and amplitude.

4. Within a given patch, the surface temperature can be varied from point to point.

5. Vertical cross section isotherms under a specified line across the ground surface can be studied.

6. Heat-flux under specified surface segments can be calculated and averaged.

Fig. 3 illustrates results using the HEATPATCH program to show the annual and monthly temperature variation under six houses adjacent to a forest, the site plot of which is shown in Fig. 1. For this calculation, it was assumed that the 20 ft by 20 ft (6.1 m by 6.1 m) slab was over earth having thermal diffusivity of 0.025 ft^2/hr (0.056 m^2/day) and undergoing an annual cyclical temperature variation with an average of $T_B = 70°F$ (21.1°C) and amplitude of $T_C = 5°F$ (2.78 K). The undisturbed or outdoor surface would undergo an annual cycle having an average temperature of $T_g = 56°F$ (13.3°C) and an amplitude of $T_A = 20.6°F$ (11.44 K). The forest temperature was assumed to undergo an annual cycle with the same annual temperature as the undisturbed exposed surface but with a much smaller amplitude of 10°F (5.55 K). The temperature profiles similar to those in Fig. 3 could also be determined for a plane normal to the earth surface and passing through any line on the surface.

Delsante Solution

Recently Delsante solved the slab-on-grade heat loss problem by applying the Fourier transform for the heat differential equation, as follows:[9]

$$\tilde{T}(x,y,z,t) = \frac{e^{i\omega}}{(2\pi)^2} \int_{-\infty}^{\infty}\int_{-\infty}^{\infty} e^{-i(ux+vy)}\, e^{-\sqrt{u^2+v^2+\lambda^2}}\, g(u,v)\,du\,dv \qquad (13)$$

where

$$g(u,v) = \int_{-\infty}^{\infty}\int_{-\infty}^{\infty} e^{i(ux+vy)}\ T(x,y,o)dxdy$$

and

$$\lambda = \sqrt{\frac{i\omega}{\alpha}} \tag{14}$$

By differentiating this temperature equation with respect to depth, Delsante obtained a closed form analytical expression for the integrated average floor heat loss as follows:

$$\tilde{q} = -k \iint_S \left.\frac{\partial T}{\partial z}\right]_{z=o} dxdy = \frac{-k}{(2\pi)^2} \int_{-\infty}^{\infty}\int_{-\infty}^{\infty} -\sqrt{u^2+v^2+\lambda^2}\ e^{-i(ux+vy)}\ g(u,v)\ dudv \tag{15}$$

Delsante's solution for an infinitely long slab of width 2b and perimeter thickness of 2ε is (Fig. 2):

$$\tilde{q} = \frac{k(\tilde{T}_1-\tilde{T}_2)}{\pi\lambda\varepsilon}\left\{\frac{\pi}{4} - K_{I_1}(2\lambda\varepsilon) + K_{I_3}(2\lambda\varepsilon) - K_{I_1}(2\lambda b) + K_{I_3}(2\lambda b) + K_{I_1}[2\lambda(b+\varepsilon)] - K_{I_3}[2\lambda(b+\varepsilon)]\right\} + 2b\lambda k\tilde{T}_1 \tag{16}$$

where

$\tilde{T}_1$ and $\tilde{T}_2$ are the Fourier transform of the slab temperature and natural or outdoor surface temperature, and K_{I_1} and K_{I_3} are integrals of modified Bessel functions K_o, so that

$$K_{I_r}(x) = \int_x^{\infty} K_{I_{r-1}}(t)dt$$

and (17)

$$K_{I_1}(x) = \int_x^{\infty} K_o(t)dt$$

In order to evaluate the complex formulation of Eq 16, a perimeter heat loss function (PHLF) I is introduced and approximated as follows:

$$I(\bar{z}) = [\frac{\pi}{4} - K_{I_1}(\bar{z}) + K_{I_3}(\bar{z})]/\bar{z}\pi$$

$$\approx \frac{1}{\pi}\left\{[-\ln\bar{z} + \delta + \frac{\pi}{4}\bar{z} + \frac{\bar{z}^2}{12}[\ln\bar{z} - (\delta + 7/3)] + \frac{\bar{z}^4}{960}[\ln\bar{z} - (\delta + \frac{61}{30})] + \frac{\bar{z}^6}{80640}[\ln\bar{z} - (\delta + \frac{457}{210})] + \frac{\bar{z}^8}{9289728}[\ln\bar{z} - (\delta + \frac{589}{252})]\right\} \tag{18}$$

where

$$\delta = \ln 2 - \gamma$$

γ in the above expression is the Euler constant (0.5772).

By substituting Eq 18 into Eq 16 and rearranging the terms, one attains a dimensionless perimeter heat loss equation:

$$\phi = \frac{\tilde{p}}{2k(\tilde{T}_1 - \tilde{T}_2)} = I(2\lambda\varepsilon) + \frac{b}{\varepsilon} I(2\lambda b) - \frac{b+\varepsilon}{\varepsilon} I(2\lambda b + 2\lambda\varepsilon)$$

or by letting $\theta_1 = 2\lambda\varepsilon$, $\theta_2 = 2\lambda(b+\varepsilon)$, and $\theta_3 = 2\lambda b$

$$\phi = \frac{\tilde{q}}{2k(T_1 - T_2)} = I(\theta_1) - I(\theta_2) + \frac{b}{\varepsilon} [I(\theta_3) - I(\theta_2)] \tag{19}$$

Under the steady-state condition, $\lambda \to 0$ and

$$\phi_\infty = \frac{\tilde{q}}{2k(\tilde{T}_1 - \tilde{T}_2)} = \frac{1}{\pi}\left\{ \ln\left(\frac{b+\varepsilon}{\varepsilon}\right) + \frac{b}{\varepsilon} \ln\left(\frac{b+\varepsilon}{b}\right)\right\} \tag{20}$$

Eq 18, however, becomes divergent for large $|\bar{z}|$. For $|\bar{z}| \geq 3$, a recommended formula for $I(\bar{z})$ is

$$I(\bar{z}) = \frac{1}{4\bar{z}} \tag{21}$$

Eq 19 represents dimensionless slab heat-transfer from a very wide and infinitely long slab for a very thin perimeter width, 2ε. To see the effect of higher harmonics influencing the perimeter floor heat loss, a complex plane representation of $I(z)$ is shown in Fig. 4 for various cyclic periods, T', when the soil thermal diffusivity is 0.025 ft^2/hr (0.56 m^2/hr) and the perimeter thickness is 1 ft (0.3 m). As the cyclic period decreases from the annual cycle to the hourly cycle, both imaginary and real components of $I(\bar{z})$ approach 0. The absolute value of the floor heat-flux for a given cyclic period T' is the vector connecting the point at a given T' on the curve in Fig. 4 and the origin. The angle of the vector indicates the phase relationship between the temperature and the heat-flux cycle. This figure clearly shows that the daily outdoor temperature cycle (T' = 24 hrs) has a relatively small impact on floor heat-transfer compared to the annual cycle.

Fig. 5 shows Eq 19 on a complex plane for a 20 ft (6.1 m) wide and infinitely long slab floor with a fixed soil thermal diffusivity and various perimeter thicknesses. The figure indicates that the complex component of the heat-flux disappears as T' approaches infinity, $\lambda \to 0$, leaving only the real and steady-state component which is expressed by Eq 20.

The above solution is applicable only to an extremely long floor slab, which is without the corner effect of the rectangular slab. Delsante also evaluated Eq 15 for a rectangular slab, such as shown in Fig. 6. In this calculation he assumed that the rectangular slab was divided into five zones: one core zone and four perimeter zones. While the slab temperature $T(x,y,o)$ is assumed constant at an indoor temperature throughout the core zone A, it varies linearly from the indoor temperature to outdoor temperature in the four perimeter zones, I through IV. The steady-state solution will be obtained by the following integral:

$$q = \frac{2k}{\pi}\int_{\infty}^{\infty}\int_{\infty}^{\infty}\sqrt{\frac{(a-u)^2+(b-v)^2}{(a-u)(b-v)}}\, T(u,v)\,du\,dv \tag{22}$$

which can be derived from Eq 15 by setting $\lambda \to 0$.

Using the surface temperature profile T(x,y,o) as shown in Fig. 2, this integral was evaluated, results of which are shown in Eqs 23, 24, 25, and 26 in four different ways as ϕ_1 through ϕ_4.

Steady-State Solution I

$$q = -k\int_{-b}^{b}\int_{-a}^{a}\left[\frac{\partial T(x,y,z)}{\partial z}\right]_{z=0} dxdy$$

$$= \frac{2k}{\pi}\int_{-\infty}^{\infty}\int_{-\infty}^{\infty}\sqrt{\frac{(a-u)^2+(b-v)^2}{(a-u)(b-v)}}\,T(u,v)dudv = \phi_1(\bar{T}_1-\bar{T}_2)$$

$$\phi_1 = \frac{2k}{\pi}G(a,b,\varepsilon) \qquad (23)$$

where

$$G(a,b,\varepsilon) = \left(2+\frac{a+b}{\varepsilon}\right)\sqrt{(a+\varepsilon)^2+(b+\varepsilon)^2}$$

$$-\sqrt{2}\left(1+\frac{a}{2\varepsilon}\right)\sqrt{a^2+(a+2\varepsilon)^2}$$

$$-\sqrt{2}\left(1+\frac{b}{2\varepsilon}\right)\sqrt{b^2+(b+2\varepsilon)^2}$$

$$-\frac{(a+b)}{\varepsilon}\sqrt{a^2+b^2}$$

$$+\frac{a^2+b^2}{\varepsilon}\left[1+\sqrt{2}\,\sinh^{-1}(-1)\right]$$

$$+2\varepsilon\left[\sqrt{2}+\sinh^{-1}(-1)\right]$$

$$-\sqrt{2}\,\frac{(a-b)^2}{\varepsilon}\left[\sinh^{-1}\left(\frac{a+b+2\varepsilon}{a-b}\right)-\sinh^{-1}\left(\frac{a+b}{a-b}\right)\right]$$

$$+\frac{(a-b)^2-(b+\varepsilon)^2}{\varepsilon}\sinh^{-1}\left(\frac{b+\varepsilon}{a+\varepsilon}\right)$$

$$+\frac{(a-b)^2-(a+\varepsilon)^2}{\varepsilon}\sinh^{-1}\left(\frac{a+\varepsilon}{b+\varepsilon}\right)$$

$$+\frac{a(2b-a)}{\varepsilon}\sinh^{-1}\left(\frac{b}{a}\right)$$

$$+\frac{b(2a-b)}{\varepsilon}\sinh^{-1}\left(\frac{a}{b}\right)$$

$$- \frac{(a^2-\varepsilon^2)}{\varepsilon} \sin h^{-1}\left(\frac{\varepsilon}{a+\varepsilon}\right)$$

$$- \frac{(b^2-\varepsilon^2)}{\varepsilon} \sin h^{-1}\left(\frac{\varepsilon}{b+\varepsilon}\right)$$

$$- (2a+\varepsilon)\sin h^{-1}\left(\frac{a+\varepsilon}{\varepsilon}\right)$$

$$+ (2b+\varepsilon)\sin h^{-1}\left(\frac{b+\varepsilon}{\varepsilon}\right)$$

$$+ \sqrt{2}\,\frac{a^2}{\varepsilon} \sin h^{-1}\left(\frac{a+2\varepsilon}{a}\right)$$

$$+ \sqrt{2}\,\frac{b^2}{\varepsilon} \sin h^{-1}\left(\frac{b+2\varepsilon}{b}\right)$$

Steady-State Solution II

when $a \gg \varepsilon$ and $b \gg \varepsilon$,

$$\phi_2 = \frac{4k}{\pi}\left[a \ln\left(\frac{2a}{\varepsilon}\right) + b \ln\left(\frac{2b}{\varepsilon}\right) + 2\sqrt{a^2+b^2} - b \sin h^{-1}\left(\frac{b}{a}\right) - a \sin h^{-1}\left(\frac{a}{b}\right)\right] \qquad (24)$$

Steady-State Solution III

$$q = -k\int_{-b-2\varepsilon}^{b+2\varepsilon}\int_{-a-2\varepsilon}^{a+2\varepsilon} \left.\frac{\partial T(x,y,z)}{\partial z}\right]_{z=0} dxdy$$

$$q = \frac{2k}{\pi}\int_{-\infty}^{\infty}\int_{-\infty}^{\infty} \sqrt{\frac{(a'-u)^2+(b'-v)^2}{(a'-u)(b'-v)}}\, T(u,v)dudv = \phi_3(\overline{T}_1-\overline{T}_2)$$

where

$a' = a+2\varepsilon$

$b' = b+2\varepsilon$

$$\phi_3 = \frac{2k}{\pi}\,(H_A+H_I+H_{II}+H_{III}+H_{IV}) \qquad (25)$$

where

$$H_A = 4\left[\sqrt{(a+\varepsilon)^2+(b+\varepsilon)^2} - \sqrt{(a+\varepsilon)^2+\varepsilon^2} - \sqrt{(b+\varepsilon)^2+\varepsilon^2} + \sqrt{2}\varepsilon\right]$$

$$+ 2(a+\varepsilon)\left[\sin h^{-1}\left(\frac{a+\varepsilon}{\varepsilon}\right) - \sin h^{-1}\left(\frac{a+\varepsilon}{b+\varepsilon}\right)\right]$$

$$+ 2(b+\varepsilon)\left[\sinh^{-1}\left(\frac{b+\varepsilon}{\varepsilon}\right) - \sinh^{-1}\left(\frac{b+\varepsilon}{a+\varepsilon}\right)\right]$$

$$+ 2\varepsilon\left[\sinh^{-1}\left(\frac{\varepsilon}{b+\varepsilon}\right) + \sinh^{-1}\left(\frac{\varepsilon}{a+\varepsilon}\right) - 2\sinh^{-1}(1)\right]$$

$$H_I = [\sinh^{-1}(1) - \sqrt{2}]\varepsilon + \left(\frac{a'^2}{\varepsilon} - \varepsilon\right)\sinh^{-1}\left(\frac{\varepsilon}{a+\varepsilon}\right) + \frac{2a'^2\alpha}{\varepsilon}$$

where

$$\alpha = \frac{1}{2} - \frac{1}{\sqrt{2}}\sinh^{-1}(1) + \frac{2-X_o}{X_o^2+2X_o-1} + \frac{2-6X_o}{(X_o^2+2X_o-1)^2}$$

$$- \frac{1}{\sqrt{8}}\ln\left(\frac{X_o+1-\sqrt{2}}{X_o+1+\sqrt{2}}\right)$$

$$X_o = \left(\frac{\varepsilon}{a+\varepsilon}\right) + \sqrt{\left(\frac{\varepsilon}{a+\varepsilon}\right)^2 + 1}$$

$$H_{II} = (\sinh^{-1}(1) - \sqrt{2})\varepsilon + \left(\frac{b'^2}{\varepsilon} - \varepsilon\right)\sinh^{-1}\left(\frac{\varepsilon}{b+\varepsilon}\right) + \frac{2b'^2}{\varepsilon}\beta$$

where

$$\beta = \frac{1}{2} - \frac{1}{\sqrt{2}}\sinh^{-1}(1) + \frac{2-X_o'}{X_o'^2+2X_o'-1} + \frac{2-6X_o'}{(X_o'^2+2X_o'-1)^2}$$

$$- \frac{\sqrt{2}}{4}\ln\frac{(X_o'+1-\sqrt{2})}{X_o'+1+\sqrt{2}}$$

and

$$X_o' = \left(\frac{\varepsilon}{b+\varepsilon}\right) + \sqrt{\left(\frac{\varepsilon}{b+\varepsilon}\right)^2 + 1}$$

$$H_{III} = J_{II} + \varepsilon\sinh^{-1}\left(\frac{b'}{\varepsilon} - 1\right) + \frac{2b'^2}{\varepsilon}\left[\ln\left(\frac{X_1-1}{X_1+1}\right) - \frac{3}{\sqrt{8}}\ln\left(\frac{X_1+1-\sqrt{2}}{X_1+1+\sqrt{2}}\right)\right.$$

$$\left. - \frac{X_1}{(X_1^2+2X_1-1)} + \frac{6X_1-2}{(X_1^2+2X_1-1)^2}\right]$$

where

$$X_1 = \left(\frac{b'-\varepsilon}{\varepsilon}\right) + \sqrt{\left(\frac{b'-\varepsilon}{\varepsilon}\right)^2 + 1}$$

if, $a' \neq b'$ then $J_{II} = b' \quad \frac{(b'-a')}{\varepsilon}\left\{ a'L_{II}+(a'-b')L_I \right\}$

if, $a' = b'$, then $J_{II} = \left\{ \sqrt{2} - \sin h^{-1}(1) \right\} \varepsilon = J_{III}$

where

$$L_{II} = \left(\frac{a'-\varepsilon}{a'-b'}\right) \ln X_2 - \left(\frac{a'}{a'-b'}\right)\ln X_1 + \ln\left\{\frac{X_2-1}{X_2+1} \cdot \frac{X_1+1}{X_1-1}\right\}$$

$$+ \frac{2(1-X_2)}{X_2^2+2X_2-1} - \frac{2(1-X_1)}{X_1^2+2X_1-1}$$

$$+ \sqrt{2} \ln\left(\frac{X_1+1-\sqrt{2}}{X_1+1+\sqrt{2}} \cdot \frac{X_2+1+\sqrt{2}}{X_2+1-\sqrt{2}}\right)$$

$$L_I = \frac{-(a'-\varepsilon)^2 \ln X_2 + a'^2 \ln X_1}{2(a'-b')^2}$$

$$- 3\,\frac{\sqrt{2}}{4} \ln\left(\frac{X_1+1-\sqrt{2}}{X_1+1+\sqrt{2}} \cdot \frac{X_2+1+\sqrt{2}}{X_2+1-\sqrt{2}}\right)$$

$$- \frac{X_1}{X_1^2+2X_1-1} + \frac{X_2}{X_2^2+2X_2-1}$$

$$- \ln\left(\frac{X_1+1}{X_1-1} \cdot \frac{X_2-1}{X_2+1}\right)$$

$$- \frac{2-6X_1}{(X_1^2+2X_1-1)^2} + \frac{2-6X_2}{(X_2^2+2X_2-1)^2}$$

and

$$X_1 = -\left(\frac{b'}{a'}\right) + \sqrt{\left(\frac{b'}{a'}\right)^2 + 1}$$

$$X_2 = -\left(\frac{b'-\varepsilon}{a'-\varepsilon}\right) + \sqrt{\left(\frac{b'-\varepsilon}{a'-\varepsilon}\right)^2 + 1}$$

$$H_{IV} = J_{III} + \varepsilon \sin h^{-1}\left(\frac{a'}{\varepsilon} - 1\right) + \frac{2a'^2}{\varepsilon}\left[\ln\left(\frac{Y_1-1}{Y_1+1}\right)\right.$$

$$- 3\,\frac{\sqrt{2}}{4}\,\ln\left(\frac{Y_1+1-\sqrt{2}}{Y_1+1+\sqrt{2}}\right) - \frac{Y_1}{Y_1^2+2Y_1-1} + \frac{6Y_1-2}{(Y_1^2+2Y_1-1)^2}$$

where

$$Y_1 = \left(\frac{a'}{\varepsilon} - 1\right) + \sqrt{\left(\frac{a'}{\varepsilon} - 1\right)^2 + 1}$$

$$J_{III} = \frac{2(a'-b')}{\varepsilon}\left(b'M_{II}+(b'-a')M_I\right)$$

where

$$Y_1 = \left(\frac{a'}{\varepsilon} - 1\right) + \sqrt{\left(\frac{a'-\varepsilon}{\varepsilon}\right)^2 + 1}$$

If $a' = b'$, then $J_{III} = \left\{\sqrt{2} - \sinh^{-1}(1)\right\}\varepsilon$

$$M_I = \frac{-(b'-\varepsilon)^2\ln Y_2+b'^2\ln Y_1}{2(b'-a')^2}$$

$$- 3\,\frac{\sqrt{2}}{4}\,\ln\left(\frac{Y_1+1-\sqrt{2}}{Y_1+1+\sqrt{2}}\cdot\frac{Y_2+1+\sqrt{2}}{Y_2+1-\sqrt{2}}\right)$$

$$- \ln\left(\frac{Y_1+1}{Y_1-1}\cdot\frac{Y_2-1}{Y_2+1}\right)$$

$$- \frac{Y_1}{Y_1^2+2Y_1-1} + \frac{Y_2}{Y_2^2+2Y_2-1}$$

$$- \frac{2-6Y_1}{(Y_1^2+2Y_1-1)^2} + \frac{2-6Y_2}{(Y_2^2+2Y_2-1)^2}$$

$$M_{II} = \frac{b'-\varepsilon}{b'-a'}\cdot\ln Y_2 - \frac{b'}{b'-a'}\ln Y_1$$

$$+ \ln\left(\frac{Y_2-1}{Y_2+1}\cdot\frac{Y_1+1}{Y_1-1}\right)$$

$$+ \frac{2(1-Y_2)}{Y_2^2+2Y_2-1} - \frac{2(1-Y_1)}{(Y_1^2+2Y_1-1)}$$

$$+ \sqrt{2} \ln \left(\frac{Y_1+1-\sqrt{2}}{Y_1+1+\sqrt{2}} \cdot \frac{Y_2+1+\sqrt{2}}{Y_2+1-\sqrt{2}} \right)$$

where

$$Y_1 = -\left(\frac{a'}{b'}\right) + \sqrt{\left(\frac{a'}{b'}\right)^2 + 1}$$

$$Y_2 = -\left(\frac{a'-\varepsilon}{b'-\varepsilon}\right) + \sqrt{\left(\frac{a'-\varepsilon}{b'-\varepsilon}\right)^2 + 1}$$

Steady-State Solution IV

A special case of solution ϕ_3 where $a' = b'$

$$\phi_4 = \frac{4k}{\pi} \left(H_A' + H_I' + H_{III}' \right) \tag{26}$$

$$H_A' = 2\left\{ \sqrt{2}a' - 2\sqrt{(a'-\varepsilon)^2+\varepsilon^2} + (a'-\varepsilon)\left[\sinh^{-1}\left(\frac{a'-\varepsilon}{\varepsilon}\right) - \sinh^{-1}(1)\right] + \varepsilon\left[\sinh^{-1}\left(\frac{\varepsilon}{a'-\varepsilon}\right) - \sinh^{-1}(1)\right]\right\}$$

$$H_I' = \left[\sinh^{-1}(1) - \sqrt{2}\right]\varepsilon + \left(\frac{a'^2}{\varepsilon} - \varepsilon\right) \sinh^{-1}\left(\frac{\varepsilon}{a'-\varepsilon}\right) + \frac{2a'^2}{\varepsilon}\,\alpha$$

where

$$\alpha = \frac{1}{2} - \frac{\sinh^{-1}(1)}{\sqrt{2}} + \frac{2-X_o}{X_o^2+2X_o-1} + \frac{2-6X_o}{(X_o^2+2X_o-1)^2} - \frac{1}{\sqrt{8}} \ln\left(\frac{X_o+1-\sqrt{2}}{X_o+1+\sqrt{2}}\right)$$

$$X_o = \left(\frac{\varepsilon}{a'-\varepsilon}\right) + \sqrt{\left(\frac{\varepsilon}{a'-\varepsilon}\right)^2 + 1}$$

$$H_{III}' = \left[\sqrt{2} - \sinh^{-1}(1) + \sinh^{-1}\left(\frac{a'-\varepsilon}{\varepsilon}\right)\right]\varepsilon + \frac{2a'^2}{\varepsilon}\,\beta$$

where

$$\beta = \ln\left(\frac{X_1-1}{X_1+1}\right) - \frac{3}{\sqrt{8}} \ln\left(\frac{X_1+1-\sqrt{2}}{X_1+1+\sqrt{2}}\right) - \frac{X_1}{X_1^2+2X_1-1} + \frac{6X_1-2}{(X_1^2+2X_1-1)^2}$$

and

$$X_1 = \left(\frac{a'-\varepsilon}{\varepsilon}\right) + \sqrt{\left(\frac{a'-\varepsilon}{\varepsilon}\right)^2 + 1}$$

While ϕ_1 is an original Delsante solution from Ref 9 which is calculated only for the area over zone A of Fig. 6, ϕ_3 was developed by the authors to include the heat loss from perimeter zones I, II, III, and IV of the slab.

The solution ϕ_2 is a special case of ϕ_1 applicable only when $a>>\varepsilon$ (a thin perimeter zone). The ϕ_4 solution is a special case of ϕ_3 when a = b (a square slab). Using these ϕ functions, thermal resistance of slab-on-grade floors of different sizes and shapes may be computed and are shown in Figs. 7 and 8. In Fig. 7 it is shown that the error caused by using simplified expression ϕ_2 in lieu of the exact formulation ϕ_1 is small unless the size is extremely small. Since ϕ_4 is extremely complex, it was used to generate correction factors for nonsquare slab heat-transfer to be applied to values determined for square slabs by ϕ_3. The correction factors correlated with respect to the hydraulic diameter $A/(\frac{P}{4})^2$ agreed extremely well with that determined by Muncy and Spencer.[5] For a large slab ($\varepsilon << a=b$), Delsante uses the following form for the calculation of floor heat loss

$$q = \mathrm{Re}\left[k_G P(\tilde{T}_1-\tilde{T}_2)L(2\lambda\varepsilon)+k_G\lambda S\tilde{T}_1\right] + \phi_4(\bar{T}_1-\bar{T}_2) \qquad (27)$$

where

Re = real part of a complex variable

k_G = soil thermal conductivity

P = slab perimeter length

S = slab area

$\tilde{T}_1, \tilde{T}_2$ = complex temperature function representing the periodic component

$\bar{T}_1, \bar{T}_2$ = average or steady part of the temperature component

Tab. 1 shows the result of comparative calculations between HEATPATCH and Delsante calculations for the steady-state heat loss ($\lambda \to 0$) from square slabs over 40 ft (12.1 m) square, as a function of perimeter zone thickness, 2ε. In this comparison, an ℓ of 6 in. (0.15 m) was used for Eq 12. Fig. 9, on the other hand, shows a similar comparison for the annual cycle of monthly floor heat-flux.

These computations were made for the annual average temperature of 56.5°F (13.5°C) and amplitude of 20.6°F (11.4 K) for the outside condition, while the average and amplitude temperature were 70°F (21.1°C) and 5°F (2.8 K), respectively, for the slab surface. Thermal conductivity of 1 Btu/hr·ft·°F (1.728 W/m·K) and thermal diffusivity of 0.025 ft^2/hr (0.056 m^2/day) were assumed for earth. The agreement between the Delsante solution and the HEATPATCH results is good, except where the perimeter thickness is either too large or too small. Another major reason for the discrepancies between the HEATPATCH solution and the Delsante solution is that the perimeter zone was considered a part of floor for the HEATPATCH calculation. While the Delsante solution is more accurate for the thin perimeter thickness, the HEATPATCH solution should reflect a more accurate picture for a wide perimeter case. As the perimeter width increases, the annual average heat loss tends to decrease and the annual amplitude of the heat loss also decreases. A most interesting aspect of the result is that heat loss from May through August is scarcely affected by the perimeter thickness. This is understandable, because the temperature profiles during that period are practically parallel to the ground surface, even near the edge, so that the heat flow should be practically normal (even over the perimeter zone) to the surface across the entire floor (see Fig. 3).

As pointed out before, the Delsante formula for the transient or periodic floor heat loss is not as exact in the steady-state case and is based upon the assumption that the three-dimensional corner effect is extremely small. Thus, it is only valid for very thin perimeter widths. On the other hand, HEATPATCH calculations yield errors due to the arbitrary nature of selecting the depth perimeter, ℓ, in Eq 12. Theoretically, the smaller the value of ℓ, the closer it will be to the exact solution.

There is, however, a problem in making the value of ℓ too small or smaller than the surface grid size Δx and Δy. As can be seen from Eq 7, the integrand L contains a variable, r, which is the distance between the earth temperature point and the differential surface segment $\Delta x \Delta y$. For the numerical calculations dealing with the finite magnitudes of Δx and Δy, this r represents the distance between the earth temperature point (x,y,ℓ) and the centroid of the surface segment (x',y',o) expressed by the following equation

$$r = \sqrt{\ell^2 + (x-x')^2 + (y-y')^2}$$

Approximation of the original integral equation by a finite difference integral (Eq 9) will be valid as long as r is considerably larger than Δx and Δy. For the small value of $z = \ell$, this criteria is difficult to meet, unless Δx and Δy are made extremely small throughout the surface region. A smaller Δx and Δy for the entire region, on the other hand, results in excessive computer time. For normal slab-on-grade heat-transfer calculations, with a floor size of more than 25 ft by 25 ft (7.6 m by 7.6 m), the smallest practical Δx and Δy is on the order of the perimeter thickness 2ε, and the depth parameter ℓ of 6 in. (0.15 m) seems to be adequate.

The floor heat loss becomes smaller as the perimeter thickness gets larger. That is, of course, partly due to the fact that the average temperature difference between the slab surface and the outdoors decreases. It is also important to note that the average floor heat flux decreases rapidly as the floor size increases, largely because the perimeter effect is lessened as the floor size increases for square slabs. The physical significance of the perimeter thickness 2ε is somewhat unclear. It has been considered as the wall thickness by Muncey[5] as well as by Delsante[9] on the assumption that the floor temperature is constant from one end of the floor to another. Under actual conditions, however, the measured floor temperature is not uniformly constant; it becomes gradually colder from the center toward the wall. In other words, the temperature transition zone is considerably wider than the wall thickness. For this reason, the HEATPATCH calculation included heat loss under the perimeter zone, since it is by definition the temperature transition zone. Unfortunately, actual magnitude of 2ε is not well known, and it varies, depending upon several factors, such as the conductivity of the floor slab, perimeter insulation, wall construction, foundation, etc. Moreover, in many cases, the type of heating system or location of heating equipment on the floor significantly affects the floor temperature distribution. In reality, the floor surface temperature is seldom maintained at a constant value when the room air temperature is controlled by the thermostat. Limited experience with NBS thermal mass test houses indicates that ℓ, or the width of the temperature transition zone, is at least 2 ft (0.61 m). The HEATPATCH program also permits the evaluation of the effect of thermal diffusivity upon the floor heat loss. It is important, however, to vary the soil thermal diffusivity together with the soil thermal conductivity, because in reality, the thermal diffusivity is directly proportional to the soil thermal conductivity.

DAILY THERMAL CYCLES

While the previous discussions are concerned with the monthly temperature and heat flow of the annual cycle, identical equations can be used to solve for the daily cycle by simply changing the value of ω from $2\pi/8760$ to $2\pi/24$. Figs. 10 and 11 compare the diurnal floor heat flux cycle with the annual cycle under identical conditions for temperature data, slab size, and soil thermal properties. Fig. 10 is for a constant indoor temperature condition and shows that the diurnal outdoor temperature cycle affects the diurnal floor heat-flux to much less of a degree than the annual temperature cycle affects the annual heat-flux. Fig. 11, on the other hand, shows that an indoor temperature fluctuation of 5°F (2.8 K) significantly affects the diurnal floor heat loss but has very little effect on the annual heat loss. The daily cycle floor heat loss is important for the consideration of solar heat absorption by the floor. To study such a situation, calculations were performed for a 10 ft by 10 ft (3.05 m by 3.05 m) section of a large floor, which is cyclically heated in such a manner that it experiences a daily maximum temperature of 130°F (54.4°C) and a minimum of 70°F (21.2°C), while the rest of the floor is maintained at 70°F (21.1°C). Using HEATPATCH, it is possible to show the distribution of heat-flux along the floor that indicates large heat-flux changes around the perimeter of the heated section. During the time that the floor was absorbing the heat, the region immediately outside the heated section was releasing the heat that was conducted into the heated section. This type of calculation should be extended to include higher harmonics to simulate the more complex diurnal surface temperature cycle representative of solar radiation incident upon the floor surface using a Fourier Series analysis. Fig. 12 is a result of such calculations for a 20 ft by 20 ft (6.1 m by 6.1 m) floor during a typical winter

day while room temperature was maintained at 70°F (21.1°C) during the day and 65°F (18.3°C) during the night. The figure shows the relationship among solar heat gain, floor heat loss, and the heat given off by the warm floor to the room during the night hours.

Conduction Transfer Functions for Composite Floor

Strictly speaking, what has been shown in the previous sections is applicable only to a bare earth floor in a house and $\tilde{T}_1$ and $\tilde{T}_2$ used in Eqs 16, 19, and 20 are essentially the surface temperatures of the earth floor and outdoors. In reality, however, a floor slab is a multilayered structure consisting of floor covering, concrete slab, insulation, subgrade gravel, etc. Moreover, the surface film heat-transfer coefficient for inside floor surface must be considered. According to Carslaw and Jaeger,[1] surface heat-flux and temperature relationship between indoor and outdoor conditions is given by the following matrix equation:

$$\begin{pmatrix} \tilde{T}_i \\ \tilde{q}_i \end{pmatrix} = \begin{pmatrix} \tilde{A} & \tilde{B} \\ \tilde{C} & \tilde{D} \end{pmatrix} \cdot \begin{pmatrix} \tilde{T}_o \\ \tilde{q}_o \end{pmatrix} \tag{28}$$

where

All the quantities with ~ denote complex variables.

If the floor system is a homogeneous plane slab of thickness ℓ, thermal conductivity k, density ρ, and specific heat c,

$$\begin{aligned} \tilde{A} &= \cos h\, \tilde{H} \\ \tilde{B} &= \frac{-R \sin h\, \tilde{H}}{\tilde{H}} \\ \tilde{C} &= \frac{-\tilde{H} \sin h\, \tilde{H}}{R} \\ \tilde{D} &= \cos h\, \tilde{H} \end{aligned} \tag{29}$$

where

$$\tilde{H} = \sqrt{i\omega RC}$$

$R = \frac{\ell}{k}$: thermal resistance

$C = \rho c \ell$: thermal capacitance

and $i = \sqrt{-1}$

If the system is purely resistive, such as the surface film having the heat-transfer coefficient h,

$$\tilde{A} = 1$$

$$\tilde{B} = -1/h$$

$$\tilde{C} = 0$$

$$\tilde{D} = 1$$

If the floor system is a multilayer composite, one can write

$$\begin{pmatrix} \tilde{A} & \tilde{B} \\ \tilde{C} & \tilde{D} \end{pmatrix} = \begin{pmatrix} \tilde{A}_1 & \tilde{B}_1 \\ \tilde{C}_1 & \tilde{D}_1 \end{pmatrix} \cdot \begin{pmatrix} \tilde{A}_2 & \tilde{B}_2 \\ \tilde{C}_2 & \tilde{D}_2 \end{pmatrix} \cdots \begin{pmatrix} \tilde{A}_n & \tilde{B}_n \\ \tilde{C}_n & \tilde{D}_n \end{pmatrix} \tag{30}$$

where

$\tilde{A}_k$, $\tilde{B}_k$, $\tilde{C}_k$, $\tilde{D}_k$, (k = 1, 2, ... n) are evaluated at each layer and post multiplied.

Using this convention, the room air to outside air floor/earth conduction system equation may be written as

$$\begin{pmatrix} \tilde{T}_I \\ \tilde{q}_I \end{pmatrix} = \begin{pmatrix} \tilde{A}_F & \tilde{B}_F \\ \tilde{C}_F & \tilde{D}_F \end{pmatrix} \cdot \begin{pmatrix} \tilde{A}_G & \tilde{B}_G \\ \tilde{C}_G & \tilde{D}_G \end{pmatrix} \cdot \begin{pmatrix} \tilde{T}_o \\ \tilde{q}_o \end{pmatrix} \tag{31}$$

where

$\tilde{A}_F$, $\tilde{B}_F$, $\tilde{C}_F$, and $\tilde{D}_F$ are for the multilayered finite-thickness floor and $\tilde{A}_G$, $\tilde{B}_G$, $\tilde{C}_G$, and $\tilde{D}_G$ are for the semi-infinite earth region around the building.

For the floor heat loss calculations, only $\tilde{B}_G$ and $\tilde{D}_G$ are needed, values of which can be determined by modifying Eq 27 as follows:

$$\tilde{B}_G = \frac{S}{P}\left(k_G\, L(2\varepsilon\lambda)\right)^{-1} \tag{32}$$

$$\tilde{D}_G = 1 + \frac{\lambda}{k_G L(2\varepsilon\lambda)}\,\frac{S}{P} \tag{33}$$

The frequency domain conduction transfer function, $\tilde{X}$ and $\tilde{Y}$, can be defined as

$$\tilde{q}_I = \tilde{X}\,\tilde{T}_I - \tilde{Y}\,\tilde{T}_o \tag{34}$$

where

$$X = -\frac{\tilde{C}_F\tilde{D}_G + \tilde{D}_F\tilde{D}_G}{\tilde{A}_F\tilde{B}_G + \tilde{B}_F\tilde{D}_G} \tag{35}$$

$$Y = \frac{1}{\tilde{A}_F\tilde{B}_G + \tilde{B}_F\tilde{D}_G} \tag{36}$$

Finally, the floor heat loss can be calculated by summing up the contribution of all the

$$q = \mathrm{Re}\sum_{i=1}^{N}\left(\tilde{X}(\omega_i)\,\tilde{T}_I(\omega_i) - \tilde{Y}(\omega_i)\,\tilde{T}_o(\omega_i)\right) \tag{37}$$

where

Re indicates that q is a real part of the complex number in the bracket. Of course, when ω_i = 0, this represents the steady-state, and $\tilde{X}$ and $\tilde{y}$ will be replaced by ϕ_2 and $\tilde{T}_I(\omega)$ and $\tilde{T}_o(\omega)$ will be replaced by T_I and T_o.

Typical values for the frequency response factors have been calculated and are shown in Tabs. 2-A and 2-B for 20 ft by 20 ft (6.1 m by 6.1 m), 30 ft by 40 ft (9.1 m by 12.2 m) and 40 ft by 50 ft (12.2 m by 15.2 m) floors. In these sample calculations a soil thermal diffusivity of 0.025 ft^2/hr (.0052 m^2/hr) and a thermal conductivity of 0.5 Btu/hr·ft·F (0.072 W/m·K) were assumed. The floor is assumed to be bare for Tab. 2-A, while Tab. 2-B is for a floor consisting of 6 in. (0.15 m) concrete and 6 in. (0.15 m) gravel above the soil.

These tables show that the Y components of the response factors are practically zero for all the frequency levels higher than the daily cycle, indicating that only the annual cyclic outdoor temperature changes affect the floor heat-transfer. The X factors are, however,

extremely large for the high frequency component, indicating that the indoor temperature fluctuation due to the thermostat daily cycle, solar beam penetration, and/or lighting schedule would have a large impact on the floor heat-transfer. Also interesting is that the X factors are virtually unaffected by a change in floor size and shape but are influenced by the floor layer structure.

SUMMARY

Using the Lachenbruch's-Green's function technique, a computer program called HEATPATCH was developed to determine underground temperature profiles under disturbed ground surface areas of various sizes and shapes. This program can also be used to compute the heat loss or heat-transfer from the disturbed regions to the undistributed ground. The heat-transfer calculation is based upon the numerical differentiation of the soil temperature near the surface. Comparison Using Delsante's exact solution shows that the temperature gradient through a 6 in. thickness of soil layer is adequate for the determination of the floor heat loss, except for the case of a very thin perimeter zone. A simplified pocket computer program was developed using Delsante's solution, which could be used as a part of the annual energy calculation if it is translated into the seasonal average subfloor temperature at 6 in. below the floor surface. Using Delsante's equation, spectral sensitivity of the floor heat loss due to shorter periodic cycles, such as the diurnal cycle, was also investigated. The diurnal floor heat loss, as affected by the daily temperature cycle, is very small. This implies that floor heat loss is basically one-dimensional or the heat flow is normal to the floor surface from center to edge as far as the hour-by-hour simulation of the building heat-transfer process is concerned. This justifies the use of the one-dimensional thermal response factor approach to determine the heat-storage effect of the floor for the hour-by-hour energy calculations. A frequency domain thermal response factor concept was developed by combining the slab floor composite with the surrounding earth. Sample response factors for typical floor construction were obtained and presented.

It is important to recognize the limitation of HEATPATCH and the Delsante solution. Both solutions do not address edge insulation. Finite-difference (FDM) and/or finite (FEM) type calculations are required to correctly account for the effect of edge insulation. The HEATPATCH technique should still be useful in expediting the FDM/FEM calculation by being able to provide accurate seasonal boundary temperature conditions under annual cyclic conditions. The HEATPATCH calculation principle also can be extended for basement wall and floor analyses but will require more complexity in keeping track of the disturbed surfaces, which will be five instead of one (for the slab-on-grade floor problem).

NOMENCLATURE

a, a'	:	half-width of slab floor, m
$\tilde{A}$	:	an element of transfer function matrix
b, b'	:	half-length of slab floor, m
$\tilde{B}$	:	an element of transfer functions matrix
c	:	specific heat, kJ/kg·K
C	:	thermal capacitance $C = \rho c \ell$, $kJ/m^2 \cdot K$
$\tilde{C}$	:	an element of transfer function matrix
$\tilde{D}$	:	an element of transfer function matrix
g	:	Fourier transform of surface temperature
H	:	a variable defined in Eq 28 in the text
i	:	complex number index, $i = \sqrt{-1}$
$l(z)$	:	perimeter function defined in Eq 18
L	:	Green's function integral

k	:	thermal conductivity, W/m•K
K_i	:	integrated Bessel function
ℓ	:	thickness of solid, m
N	:	number of temperature cycle harmonics
P	:	perimeter of the slab, m
q	:	heat flow, W
r	:	distance between the surface point and a point in the earth, m
R	:	distance between the two surface points, m
S	:	area of the slab, m^2
t and t'	:	time, hr
T	:	temperature, °C or K
T'	:	period of the temperature cycle, hr
T_A	:	amplitude of the natural or undisturbed earth surface temperature cycle, °C
T_B	:	average temperature of the slab above the annual average outdoor temperature, °C
T_C	:	amplitude of the temperature cycle for the disturbed surface, °C
T_g	:	annual average of the natural surface (outdoor) temperature cycle, °C
u	:	Fourier transform variable
v	:	Fourier transform variable
x,y,z	:	coordinate system for the subsurface point, m
x',y'	:	coordinate system for the surface point
$\tilde{X},\tilde{Y},\tilde{Z}$	:	frequency domain thermal response factors
$\bar{z}$	:	general complex variable
α	:	thermal diffusivity of earth, m^2/day
γ	:	Euler constant
δ	:	defined in Eq 18
ϵ	:	half-thickness of the perimeter zone, m
λ	:	defined in Eq 14 $=\sqrt{\frac{i\omega}{\alpha}}$
ω	:	angular frequency = $2\pi/T'$, rad/hr
ϕ	:	heat-flux function W/K
ξ	:	phase angle, radian
Ω	:	solid angle, steradian
θ	:	angle, radian
ρ	:	density kg/m^3

Subscripts

F : floor slab

G : earth or ground

I : inside the building

i : ith harmonics

k : kth layer

o : outside

∞ : undisturbed condition

Others

Variables with ~ denote complex variables

Variables with - denote average values

REFERENCES

1. H.S. Carslaw and J.C. Jaeger, Conduction of Heat in Solids (Oxford: Clarendon Press, 1946), pp 353-357.

2. H.D. Barelther, A.N. Fleming, and H.E. Alberty, "Temperature and Heat Loss Characteristics of Concrete Floors Laid on the Ground," University of Illinois Small Homes Council Technical Report, PB 93920, 1948.

3. A.H. Lachenbruch, "Three Dimensional Heat Conduction in Permafrost beneath Heated Buildings," Geological Survey Bulletin 1052-B (Washington, DC: U.S. Government Printing Office, 1957).

4. B. Adamson, "Soil Temperature under Houses without Basements," Byggforskningen Handlinger (Nr 46 Transactions, 1964).

5. R.W.R. Muncey and J.W. Spencer, "Heat Flow into the Ground under a House," Energy Conservation in Heating, Cooling, and Ventilating Buildings, Vol. 2 (Washington, DC: Hemisphere Publishing Corporation, 1978), pp. 649-660.

6. H. Akasaka, "Calculation Methods of the Heat Loss Through a Floor and Basement Walls," Transactions of the Society of Heating, Air-Conditioning, and Sanitary Engineers of Japan (No. 7, June 1978), pp. 21-35.

7. C.W. Ambrose, "Modeling Losses from Slab Floors," Building and Environment, 16:4 (1981), pp. 251-258.

8. T. Kusuda, M. Mizuno, and J. W. Bean, "Seasonal Heat Loss Calculation for Slab-on-Grade Floors," NBSIR 81-2420 (National Bureau of Standards, March 1982).

9. A.F. Delsante, A.N. Stokes, and P.J. Walsh, "Application of Fourier Transform to Periodic Heat Flow into the Ground under a Building," to be published in the International Journal of Heat and Mass Transfer.

TABLE 1
Steady-State Heat Loss
(Btu/hr)

a = b (ft)	(m)	2ε (ft)	(m)	HEATPATCH Btu/hr	W	Delsante Solution Btu/hr	W
20	6.1	0.5	0.15	2847	834	3144	921
20	6.1	1	0.30	2562	751	2608	764
20	6.1	2	0.61	1944	570	2036	597
20	6.1	5.7	1.73	944	277	1074	315
10	3.05	0.5	0.15	1128	331	1304	382
10	3.05	1	0.30	922	270	1018	298
10	3.05	1.75	0.53	734	215	769	225
10	3.05	2.85	0.87	500	147	537	157
10	3.05	4.3	1.31	319	93	335	98

TABLE 2-A
Frequency Domain Thermal Response Factors for Slab Floor

Floor Construction: Surface Resistance Bare Soil

20' x 20' slab	X	Y
3 hour cycle	1.2981 - i(0.6508)	-0.00078 - i(0.00155)
6 " "	1.1400 - i(1.0206)	-0.00243 - i(0.00273)
12 " "	0.6461 - i(1.3068)	-0.00629 - i(0.00336)
24 " "	0.05767 - i(1.1533)	-0.01109 - i(0.00151)
Annual cycle	-0.07655 - i(0.0208)	-0.04507 + i(0.01182)
Steady-state	0.09366	0.09366
30' x 40' slab	**X**	**Y**
3 hour cycle	1.2976 - i(0.6508)	-0.00045 - i(0.00090)
6 " "	1.1388 - i(1.0197)	-0.0014 - i(0.00159)
12 " "	0.6455 - i(1.3030)	-0.00366 - i(0.00195)
24 " "	0.06136 - i(1.1479)	-0.00644 - i(0.00087)
Annual cycle	0.05667 - i(0.0256)	-0.02587 + i(0.00666)
Steady-state	0.0656	0.0656
40' x 50' slab	**X**	**Y**
3 hour cycle	1.2975 - i(0.6507)	-0.00035 - i(0.00070)
6 " "	1.1384 - i(1.0194)	-0.00109 - i(0.00122)
12 " "	0.6453 - i(1.3019)	-0.00282 - i(0.00150)
24 " "	0.06253 - i(1.1461)	-0.00496 - i(0.00067)
Annual cycle	0.05045 - i(0.0270)	-0.01986 + i(0.00509)
Steady-state	0.0547	0.0547

TABLE 2-B
Frequency Domain Thermal Response Factors for Slab Floor

Surface Resistance
Floor Construction: 6" Concrete

20' x 20' slab	X	Y
3 hour cycle	0.9679 + i(0.0918)	0
6 " "	0.9264 + i(0.1169)	0
12 " "	0.8779 + i(0.1530)	-0.00011 - i(0.00026)
24 " "	0.7976 + i(0.1981)	0.00116 - i(0.00117)
Annual cycle	-0.0942 - i(0.0087)	-0.05610 + i(0.01301)
Steady-state	0.0758	0.0758
30' x 40' slab	**X**	**Y**
3 hour cycle	.9689 + i(0.0920)	0
6 " "	.9272 + i(0.1171)	0
12 " "	.8786 + i(0.1533)	0
24 " "	.7983 + i(0.1983)	0.00069 - i(0.00068)
Annual cycle	-0.0652 - i(0.0135)	-0.03040 + i(0.00653)
Steady-state	0.0564	0.0564
40' x 50' slab	**X**	**Y**
3 hour cycle	.9689 + i(0.0920)	0
6 " "	.9282 + i(0.1171)	0
12 " "	.8786 + i(0.1533)	0
24 " "	.7983 + i(0.1983)	0.00053 - i(0.00052)
Annual cycle	-.0568 - i(0.0147)	- .02292 + i(0.00481)
Steady-state	0.0481	0.0481

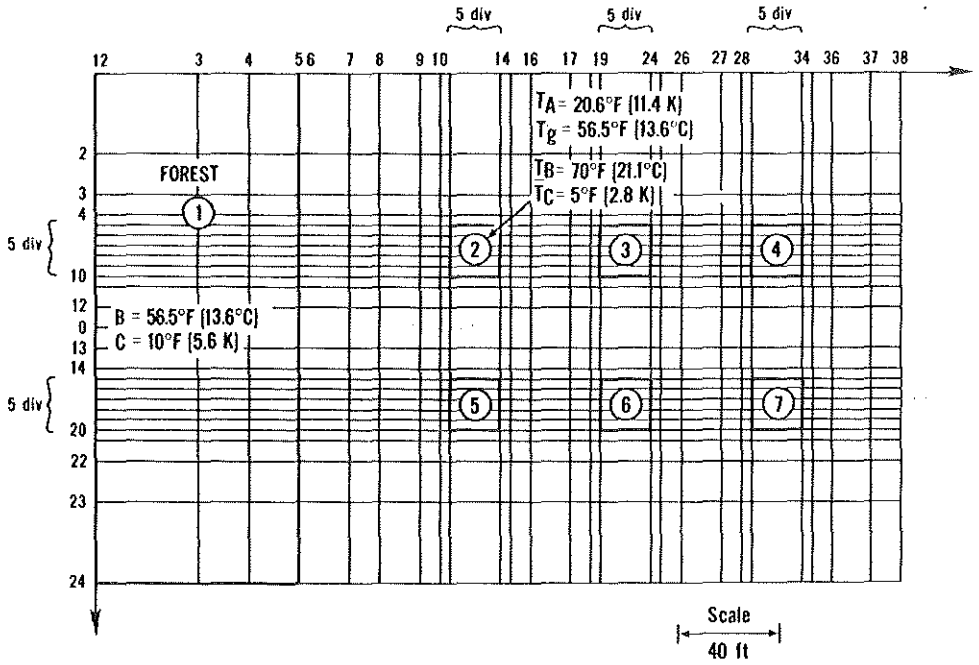

Figure 1. Surface grid design for the HEATPATCH calculation: example of six houses near a forest

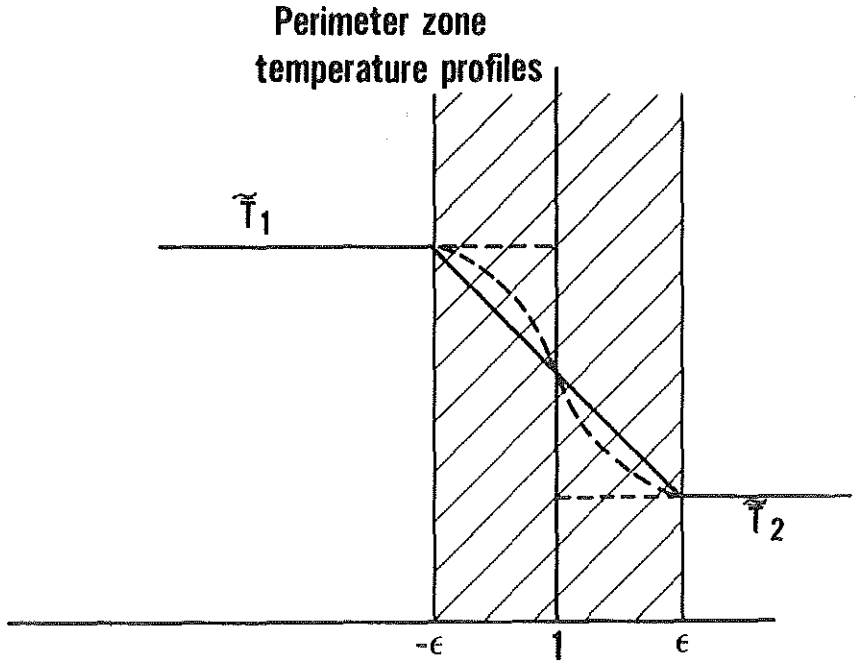

Figure 2. Temperature transition across the perimeter zone

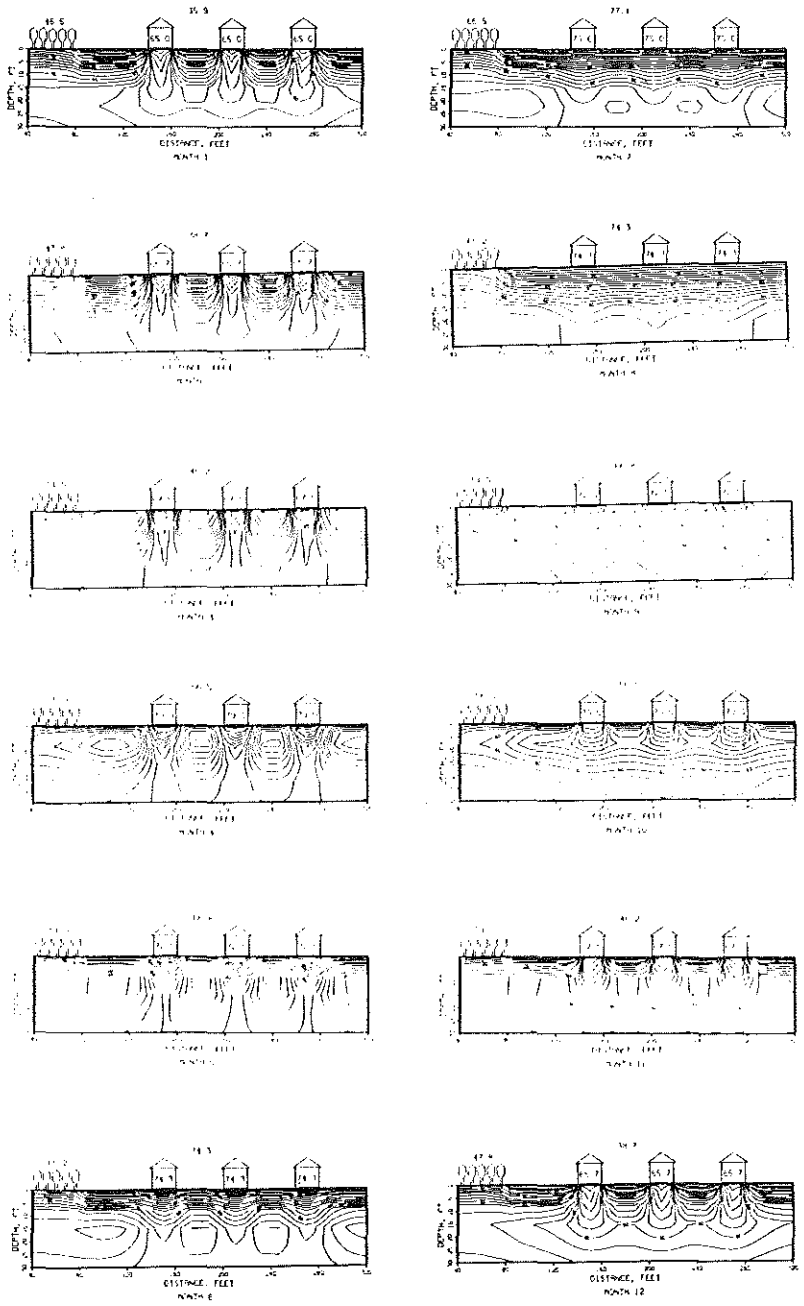

Figure 3. Monthly earth temperature profile under six houses and a forest (for site plan, see Fig. 1)

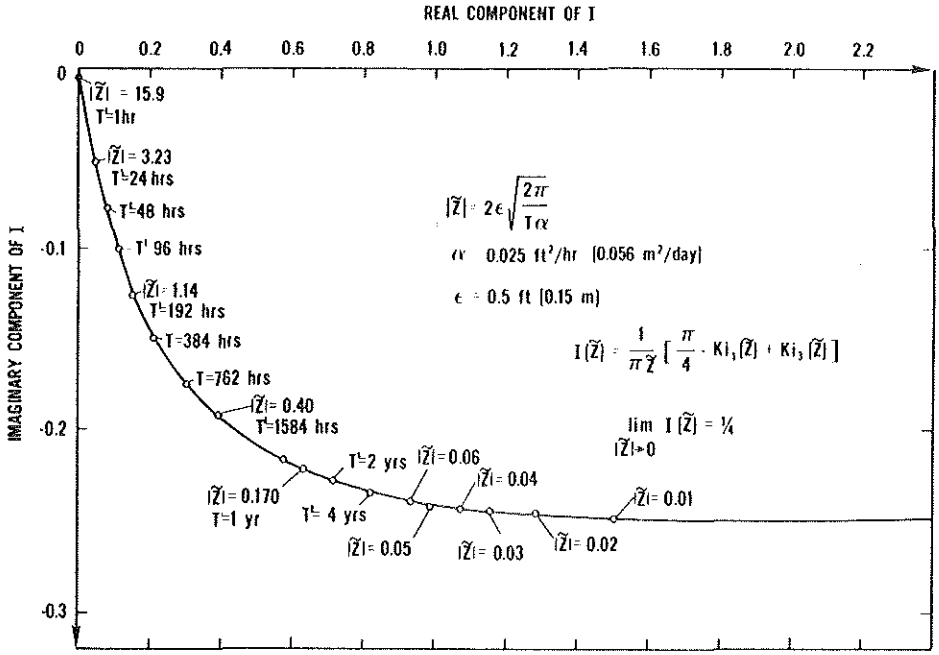

Figure 4. Two-dimensional slab-on-grade heat transfer function for very small perimeter width

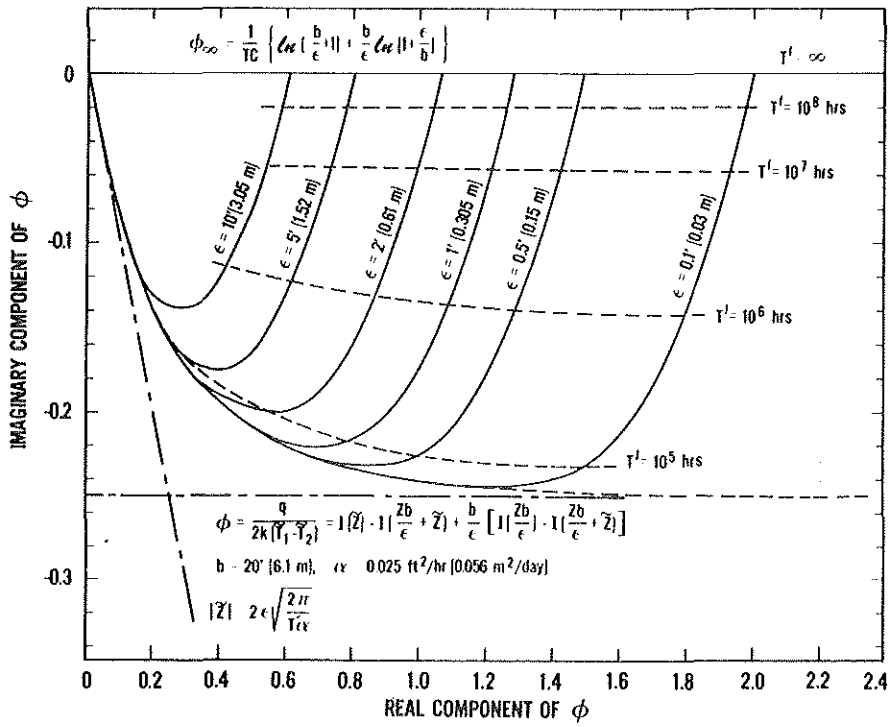

Figure 5. Two-dimensional slab heat transfer

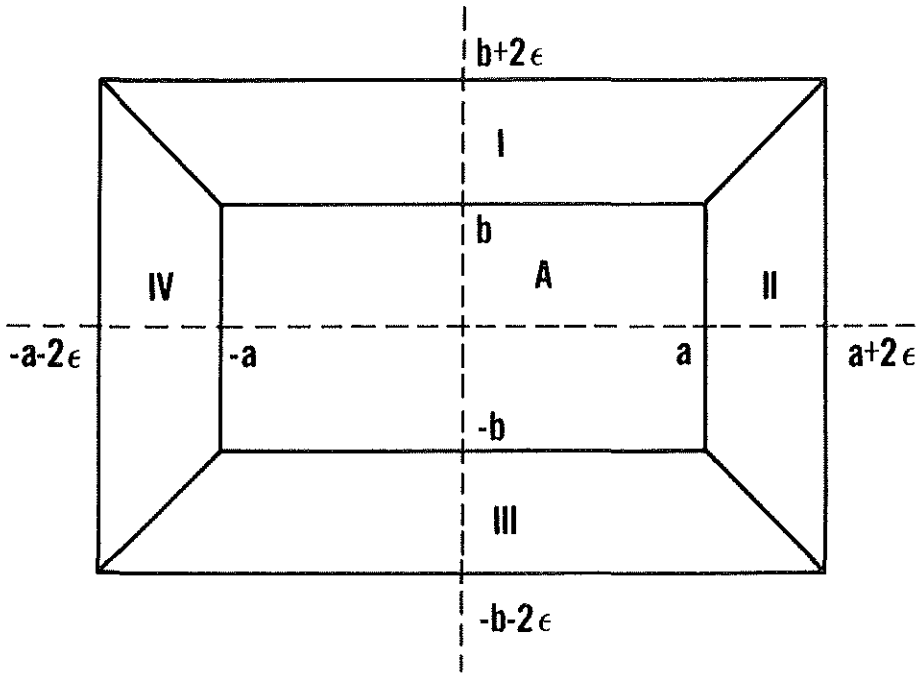

Figure 6. Rectangular slab on dimension 2a x 2b with perimeter width of 2ϵ

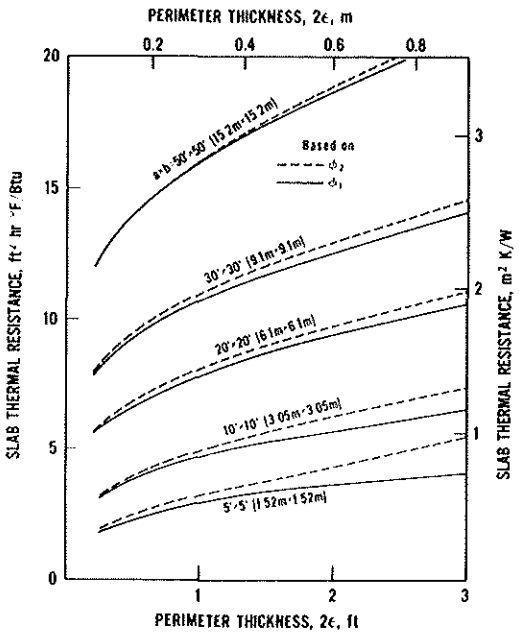

Figure 7. Thermal resistance of slab with respect to slab sizes

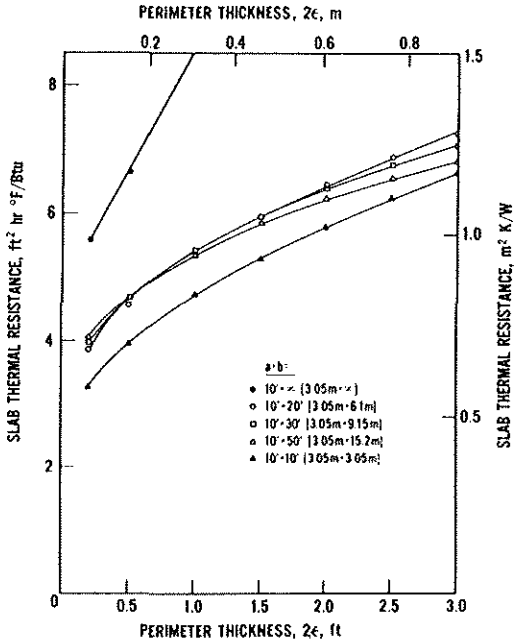

Figure 8. Thermal resistance of slab of different aspect ratios

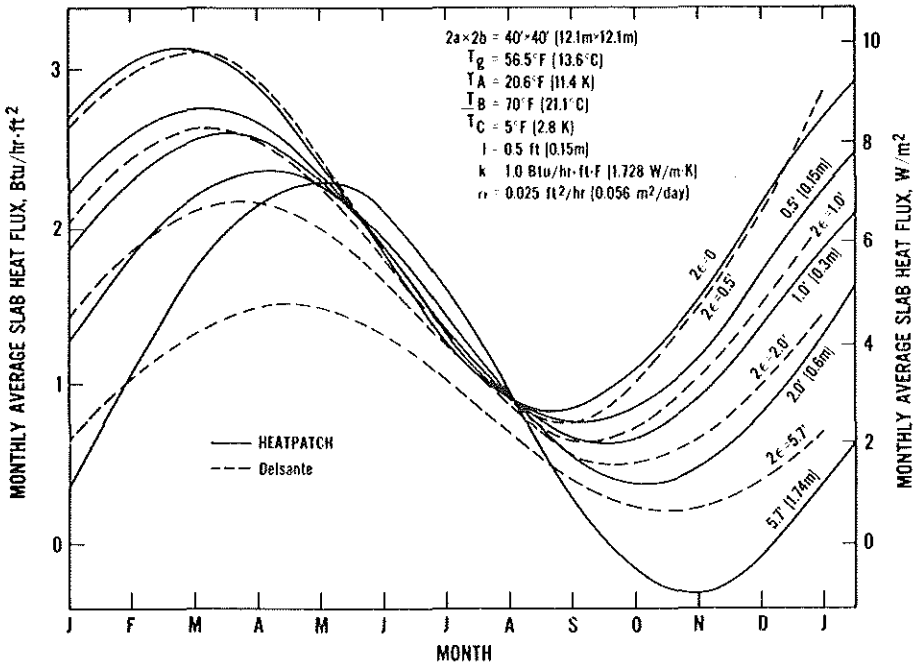

Figure 9. Annual heat flux cycle from 40 ft x 40 ft (12.1 m x 12.1 m) slab floor with different perimeter widths

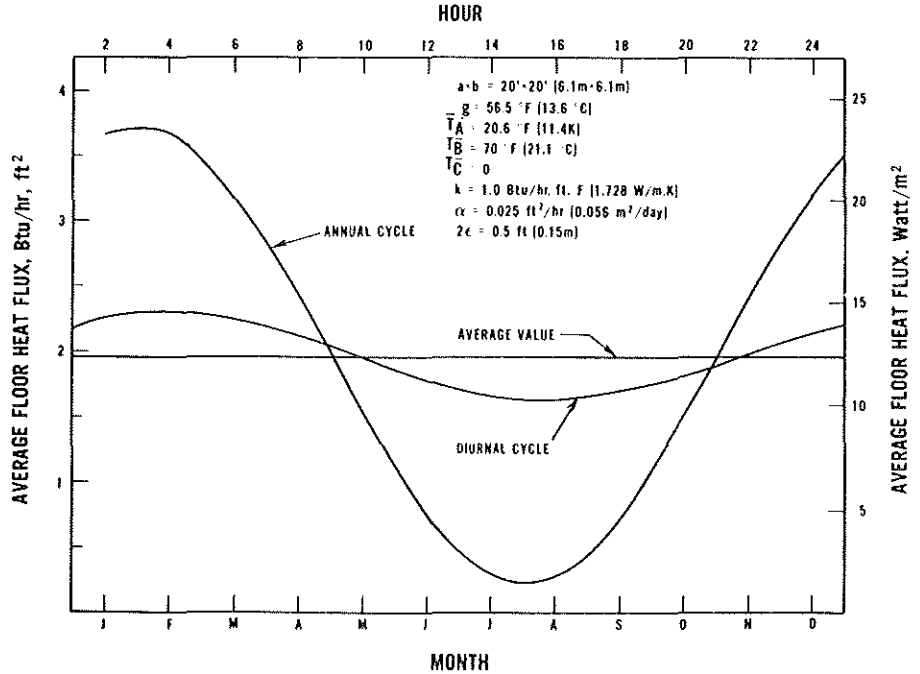

Figure 10. Comparison between the diurnal and annual heat flux cycles for slab-on-grade floor under the constant indoor temperature condition

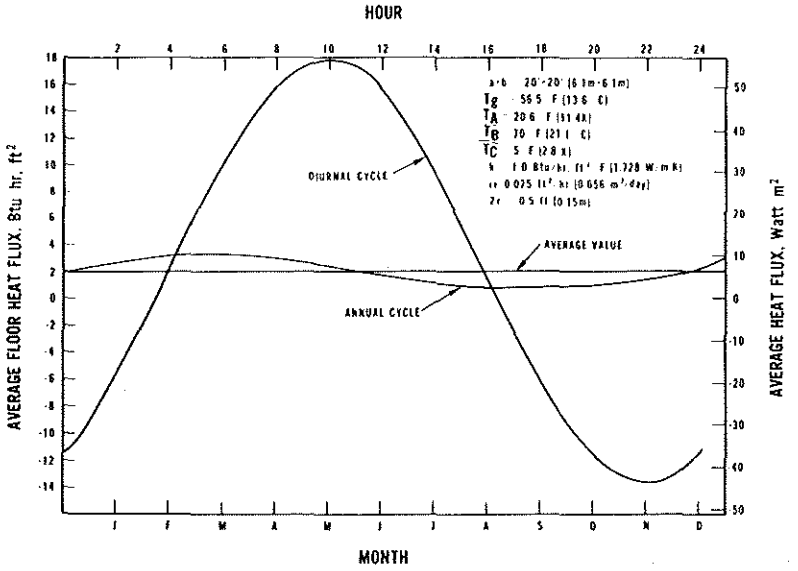

Figure 11. Comparison between the diurnal and annual heat flux cycles for slab-on-grade floor when indoor temperature fluctuates

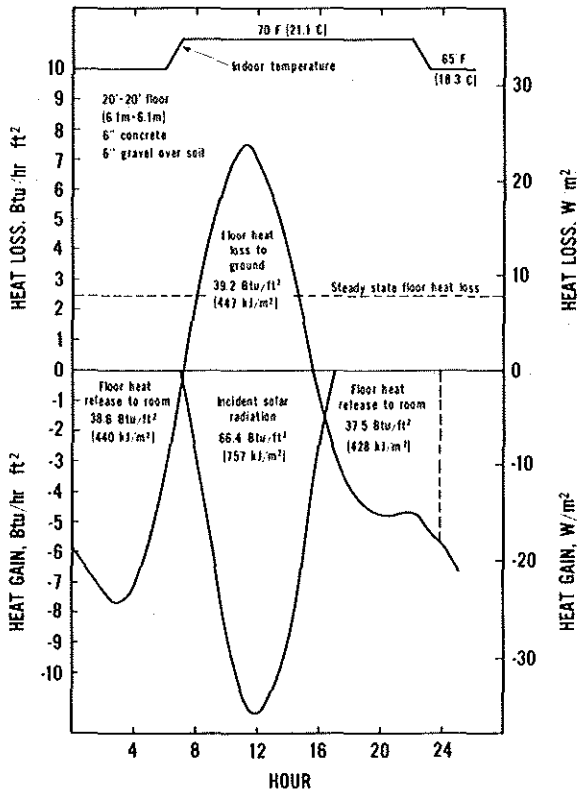

Figure 12. Diurnal floor heat flux cycle due to solar heat gain

Discussion

M. Masoero, Research Scientist, Dipartimento di Energetica, Torino, Italy: Can your method be applied to the case in which the water table is at a finite distance from the floor, thus imposing a fixed temperature boundary condition to the problem?

T. Kusuda: No, the solution is only applicable to a semi-infinite heat conduction region. The finite thickness ground system requires a different type of solution.

A. Lannus, Pgm. Mgr., EPRI, Palo Alto, CA: Would you be able to test your calculations versus experimental data from research houses from other studies using measurements of ground temperatures at various depths?

Kusuda: Yes, it is possible to compare the calculated earth temperature profile under buildings with those measured by several organizations that you referred to, although we have not done so. We have, however, compared the slab floor heat loss determined by the procedure presented herein with the data presented by one of these organizations during this conference. Relatively good agreements were obtained if we assumed the equivalent perimeter thickness of three feet.

D.W. Yarbrough, Prof. of Chem. Eng., Tennessee Tech. Univer., Cookeville: Can your method take into account variation of soil properties with position?

Kusuda: No, the solution is only valid for the honogeneous soil. The spatial variation of soil property can only be handled by the numerical technique such as the finite difference and/or finite element methods.

P.R. Achenbach, Conslt., McLean, VA: In the 1940s, NBS did some research on slab floors that reached the conclusion that the principal heat loss from a slab-on-grade floor occurred at the slab perimeter. Your presentation seemed to indicate that the predominant heat flux for an edge-insulated slab was the flux at the center of the floor. Did I understand your statements correctly?

Kusuda: What I intended to say was that the analytical procedure presented herein consists of a steady-state component that is based on the annual average earth temperature and the periodic component, which is based on the monthly variation of the earth surface temperature. The periodic component is affected by the perimeter length of the floor. When the perimeter is well insulated, only the steady-state component plays the dominant role. The calculated slab heat loss based on the steady-state component agrees well with the ASHRAE design values for the well-insulated perimeter floor.

Achenbach: Does your analytical solution permit the determination of the optimum thickness or thermal resistance of the edge insulation of a concrete slab-on-grade?

Kusuda: The analytical solution presented here cannot handle the problem of determining the optimal thickness of edge thermal insulation. It only provides the exact solution for estimating heat loss from non-edge-insulated slab floors and from perfectly-edge-insulated floors.